12th International Symposium on Turbulence and Shear Flow Phenomena (TSFP12)
Osaka, Japan, July 19–22, 2022

A SCALE-SPACE ANALYSIS OF SIMULTANEOUS ENERGY, HELICITY, AND ENSTROPHY CASCADES

Douglas W. Carter
Department of Aeronautical and
Astronautical Engineering
University of Southampton
Burgess Road, Southampton, UK SO17 1BJ
D.W.Carter@soton.ac.uk

Felipe Alves Portela
Laboratoire de Mécanique
des Fluides de Lille
University of Lille, CNRS
Kampé de Fériet, F-59000 Lille, France
felipe.alvesportela@univ-lille.fr

Paweł Baj
Institute of Aeronautics and Applied Mechanics
Warsaw University of Technology
Nowowiejska 24, 00-665 Warsaw, Poland
pawel.baj@pw.edu.pl

ABSTRACT

We characterise the incompressible turbulence cascade in terms of the concurrent inter-scale and inter-space exchanges of the scale-by-scale energy, helicity and enstrophy. The governing equations for the scale-by-scale helicity and enstrophy are derived in a similar fashion to that of the second order velocity structure function obtained by Hill (2002). We apply these equations to both forced periodic turbulence and a von Kármán flow, focusing on scales smaller than $r = \lambda$, Taylor length scales. The well-known random sweeping effect in the energy cascade between unsteady and non-linear transport is found to extend across all quantities considered. Additional mechanisms within the individual cascades are identified. Across cascades, the helicity cascade was found to be decorrelated from the others at all scales.

INTRODUCTION

The instantaneous interactions between eddies that govern turbulence are highly dynamic, taking place across a broad range of scales. The distinction between the instantaneous interactions in the turbulence and the statistically stationary cascade that they give rise to are a well known problem in turbulence modelling. For example, in Large Eddy Simulations (LES) the directionality of the cascade (from large scales to small scales, or vice-versa) at any given instant may differ from that predicted by statistically stationary models (Germano *et al.*, 1991) in which energy is transferred on average, from large, energy-containing eddies, to small, energy-dissipating ones. Recent work by Goto & Vassilicos (2016) and Yasuda & Vassilicos (2018) highlights how the statistically stationary viewpoint of the turbulence cascade effectively overlooks important dynamics that underlay (and set) the stationary state itself. The present work seeks to expand upon this viewpoint using a correlation-based analysis of cascades of energy, helicity and enstrophy.

The core element at the heart of the turbulence cascade is the rate of kinetic energy dissipation $\varepsilon = 2\nu S_{ij}S_{ij}$, ν being the fluid's kinematic viscosity and S_{ij} the strain-rate tensor. This quantity lies at the center of the Richardson-Kolmogorov cascade phenomenology (Richardson, 1920; Kolmogorov, 1941*a*,*b*). Under the assumptions of local homogeneity, isotropy, and appropriate separation of scales, it balances the non-linear inter-scale energy transfer to yield the infamous Kolmogorov's 4/5-ths law. The dissipation ε is intimately linked with the enstrophy $\omega^2 = \omega_i\omega_i$ (where $\omega_i = \varepsilon_{ijk}\partial/\partial x_j u_k$ is the vorticity vector) as well as the second invariant of the NS equations known as the helicity $h = u_i\omega_i$. It is clear that a full characterisation of the turbulence cascade must involve not only the kinetic energy but also quantities such as enstrophy and helicity, as they bear relation to dissipation and capture the presence of coherence, intermittency, parity, and other such phenomena known to break with the classical picture of turbulence.

SCALE-SPACE FRAMEWORK

Hill (2002) derived a budget for the scale-space energy increment $\delta q^2 = \delta u_i \delta u_i$, where $\delta u_i = u_i - u_i'$ is the difference of the velocity at two independent points x_k and x_k'. This budget can be obtained directly from the Navier-Stokes equations without requiring any information regarding the structure of the flow, reducing to the Kármán-Howarth equation under the assumptions of homogeneity, isotropy and stationarity. An identical procedure is carried out to derive the evolution equations for the scale-space helicity $\delta h \equiv \delta u_i \delta\omega_i$ and scale-space enstrophy $\delta\omega^2 \equiv \delta\omega_i\delta\omega_i$. This results in three generalised equations capturing the instantaneous dynamics of the energy, helicity, and enstrophy (in the absence of explicit forcing) for incompressible turbulent flow:

$$\overbrace{\frac{\partial \delta q^2}{\partial t}}^{\mathscr{A}_t} + \overbrace{\boldsymbol{\nabla}_r \cdot \boldsymbol{\delta u} \delta q^2}^{\Pi} = -\overbrace{\boldsymbol{\nabla}_X \cdot \frac{\Sigma \boldsymbol{u} \delta q^2}{2}}^{\mathscr{T}} - 2\overbrace{\boldsymbol{\nabla}_X \cdot \boldsymbol{\delta u} \delta p}^{\mathscr{T}_p} + \underbrace{\nu \left(2\nabla_r^2 + \frac{1}{2}\nabla_X^2\right)\delta q^2}_{\mathscr{D}_\nu} - 2\Sigma \underbrace{\varepsilon^{q^2}}_{\mathscr{E}}, \quad (1)$$

$$\frac{\partial \delta h}{\partial t} + \nabla_r \cdot \left(\delta \boldsymbol{u} \delta h - \frac{\delta \boldsymbol{\omega} \delta q^2}{2} \right) = -\nabla_X \cdot \left(\frac{\Sigma \boldsymbol{u} \delta q^2}{2} - \frac{\Sigma \boldsymbol{\omega} \delta q^2}{4} \right) - \nabla_X \cdot \delta \boldsymbol{\omega} \delta p + \nu (2\nabla_r^2 + \frac{1}{2}\nabla_X^2) \delta h - 2\Sigma \varepsilon^h, \quad (2)$$

$$\frac{\partial \delta \omega^2}{\partial t} + \nabla_r \cdot \delta \boldsymbol{u} \delta \omega^2 = -\nabla_X \cdot \frac{\Sigma \boldsymbol{u} \delta \omega^2}{2} + \langle \delta \boldsymbol{\omega} \delta \boldsymbol{\omega}^T, \Sigma \boldsymbol{S} \rangle + \langle \delta \boldsymbol{\omega} \Sigma \boldsymbol{\omega}^T, \Sigma \boldsymbol{S} \rangle + \nu \left(2\nabla_r^2 + \frac{1}{2}\nabla_X^2 \right) \delta \omega^2 - 2\Sigma \varepsilon^\omega. \quad (3)$$

In eqs. (1) to (3) the symbol Σ indicates the two-point sum (akin to the two-point difference δ), angled brackets denote the inner product, $\boldsymbol{S}$ is the strain-rate tensor, p is the ratio of pressure to (constant) density, ν is the kinematic viscosity and ε is the viscous dissipation of the quantity in the superscript. The gradient operator corresponds to gradients with respect to the scale variable r_i and the centroid position X_i (Mollicone *et al.*, 2018). The shorthand notation for the various transfers in equation 1 apply analogously to equations 2 and 3, with the exception that the generation terms of equation 3 appear in lieu of the pressure transport with the shorthand $\mathscr{G}_S = \langle \delta \boldsymbol{\omega} \delta \boldsymbol{\omega}^T, \Sigma \boldsymbol{S} \rangle + \langle \delta \boldsymbol{\omega} \Sigma \boldsymbol{\omega}^T, \Sigma \boldsymbol{S} \rangle$.

Notice that these three budgets are similarly structured. $\mathscr{A}_t$ is an unsteady term and represents the temporal increase or decrease of energy/helicity/enstrophy at each instant and at each scale. Π represents the nonlinear transfer in scale space. It describes the transfer of energy/helicity/enstrophy from a spherical shell at scale r_k centred on X_k to either an adjacent shell or to an adjacent location within the same shell $r_k + \mathrm{d}r_k$. $\mathscr{T}$ is the nonlinear turbulent transport in physical space. It captures the transport of energy/helicity/enstrophy from a spherical shell of radius r_k centred at X_k to an adjacent spherical shell at the same r_k centred at $X_k + \mathrm{d}X_k$. $\mathscr{T}_p$ results from the interaction of the pressure and velocity/vorticity fields to produce a pressure transport (similar to $\mathscr{T}$) that acts to transport energy/helicity at a particular scale to a neighboring shell. $\mathscr{G}_S$ is a generation term in scale space resulting from the coupling between the rate-of-strain and the enstrophy. $\mathscr{D}_\nu$ represents the viscous diffusion of energy/helicity/enstrophy in scale space and physical space. $\mathscr{E}$ represents the two-point average dissipation rate. This can be seen, for example for the scale to scale energy transfers, dividing equation 1 by 4 on both sides such that $\mathscr{E} = \frac{1}{2}(\varepsilon + \varepsilon')$ where $\varepsilon = \nu(\partial u_i / \partial x_k)^2$.

We refer to Valente & Vassilicos (2015); Gomes-Fernandes *et al.* (2015); Alves Portela *et al.* (2017); Mollicone *et al.* (2018) who give a more detailed interpretation of transport, production and destruction terms, as such. Henceforth, superscript notation is adopted to distinguish the various transfers of energy (q^2), helicity (h), and enstrophy (ω^2).

Data Set Descriptions

The instantaneous cascades are evaluated using two data sets of homogeneous turbulence. The first is a direct numerical simulation (DNS) of homogeneous isotropic turbulence at Taylor-microscale Reynolds number $Re_\lambda = 433$ from the Johns Hopkins Turbulence Database (JHU, Li *et al.*, 2008). We analyse 2560 full resolution sub-cubes from the full simulation of side length 5λ. A separate analysis on time-resolved 3D-3C scanning particle image velocimetry data from the center of a Von-Kármán mixing tank (VK) from the work of Knutsen *et al.* (2020) was also performed for comparison, for which $Re_\lambda = 199$ and 2×10^5 snapshots were used. The experimental cubes of data are slightly smaller, with side lengths of approximately 1.5λ.

RESULTS

Characterisation of the data sets

In order to characterise the three scale-space quantities of interest, we first investigate the ensemble-averaged scale-space energy $\overline{\delta q^2}$, helicity $\overline{\delta h}$, and enstrophy $\overline{\delta \omega^2}$ structure functions for the data sets. These are shown for the VK and JHU data in figure 1. Upon appropriate normalisation (as in the figure), these functions are expected to plateau in the inertial range (beyond the Taylor microscale). The limited size of the data cubes in the experimental data set prevents us from detecting such a plateau, however there is close agreement with the larger DNS cubes that do appear to plateau at $r \gtrsim \lambda$. Finite Reynolds number effects must also be taken into account.

Despite the lack of explicit helical forcing in the DNS, the scale-space helicity is non-zero for both data sets. This is consistent with the helicity spectrum computed over a wide range of simulations (Chen *et al.*, 2003; Mininni *et al.*, 2006) with and without helical forcing (Alexakis, 2017). This can be seen directly through an expansion of $\overline{\delta h}$, i.e. for homogeneous turbulence $\overline{(u_i - u_i')(\omega_i - \omega_i')} = 2\overline{h} - 2\overline{u_i \omega_i'}$. This expansion reveals that even when small-scale mirror symmetry holds ($\overline{h} = 0$) the non-zero scale space helicity (and spectrum of helicity) arises from the coherence in the velocity-vorticity correlation (Levich & Shtilman, 1988).

We next consider the non-linear flux (NLF) structure functions for each of the cascades. A small departure to justify this chosen terminology will be taken here. These structure functions are commonly referred to as "third-order structure functions", but as the origin of "third order" is in the statistical moment of the increment of a single quantity (i.e. $\overline{\delta u^3}$) a different terminology is adopted for improved generality. As noted by Hill (2002), making use of Gauss' theorem when integrating the non-linear energy transfer term of eq. (1) over the spherical scale space volume $\mathscr{V}_r$ gives $\iiint \Pi^{q^2} d\mathscr{V}_r = \oiint_{\partial \mathscr{V}_r} \overline{\delta u_k \delta q^2} n_k d\mathscr{S}$ with n_k the outward normal vector and $d\mathscr{S}$ the surface of the spherical shell. The orientation average over the spherical shell is identically zero, leaving only a flux in the radial direction. This motivates referring to these quantities as non-linear flux (NLF) structure functions in the present context. In addition to the central role of NLF structure functions in classical turbulence theory, i.e. the 4/5ths (K41) and 2/15ths laws (Chkhetiani, 1996; L'vov *et al.*, 1997), their physical significance is well documented in the context of a spherical scale-space coordinate system (Valente & Vassilicos, 2015; Gomes-Fernandes *et al.*, 2015; Alves Portela *et al.*, 2017).

The orientation-averaged NLF energy structure function is shown in fig. 2(a) normalised using the classical 4/3rds law (a form of the 4/5ths law that avoids breaking down δq^2 into components, see Hill, 2002). The subscript "r" is used to denote the radial flux in the spherical coordinate system. The plateau seen in the JHU data, for scales beyond the Taylor microscale, suggests classical behavior of $\overline{\delta u_r \delta q^2}$. Consistent with fig. 1, the VK data does not show a clear plateau developing for $\overline{\delta u_r \delta q^2} / \frac{4}{3} \varepsilon^{q^2} r$, but does reach a maximum value close to one at $r \approx \lambda$.

The orientation-averaged NLF helicity structure functions are shown in figures 2(b) and 2(c) normalised using the product of r and dissipation rate of helicity ε^h. This normalisation is chosen to compare the two distinct mechanisms associated with Π^h in equation 2. The first, $\overline{\delta u_k \delta h}$, originates from the advective term and the second, $\overline{\delta \omega_k \delta q^2}$, from the vortex stretching term of the vorticity form of Navier-Stokes equations (Yan *et al.*, 2019). It is again seen that, due to its non-positive definiteness and inherently high variation, the non-

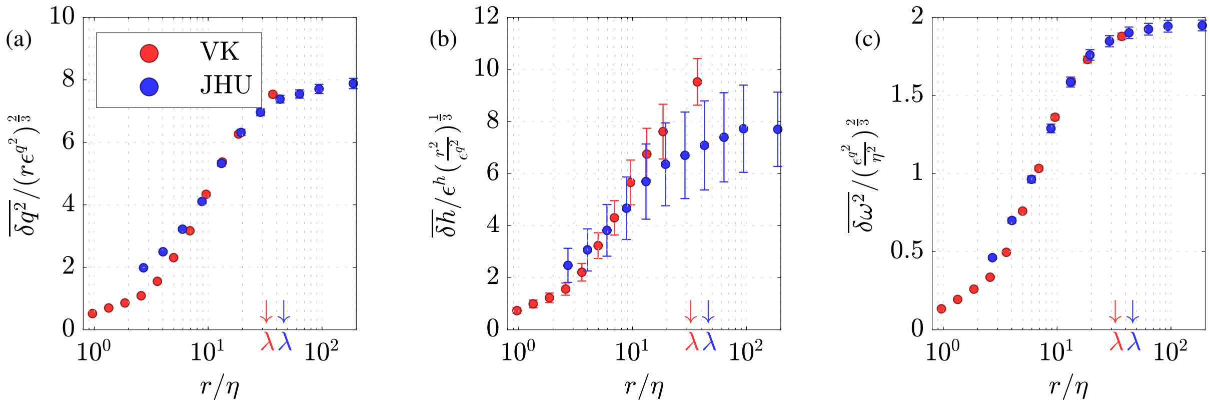

Figure 1: Normalized mean energy structure function $\overline{\delta q^2}$ (a), helicity structure function $\overline{\delta h}$ (b), and enstrophy structure function $\overline{\delta \omega^2}$ (c).

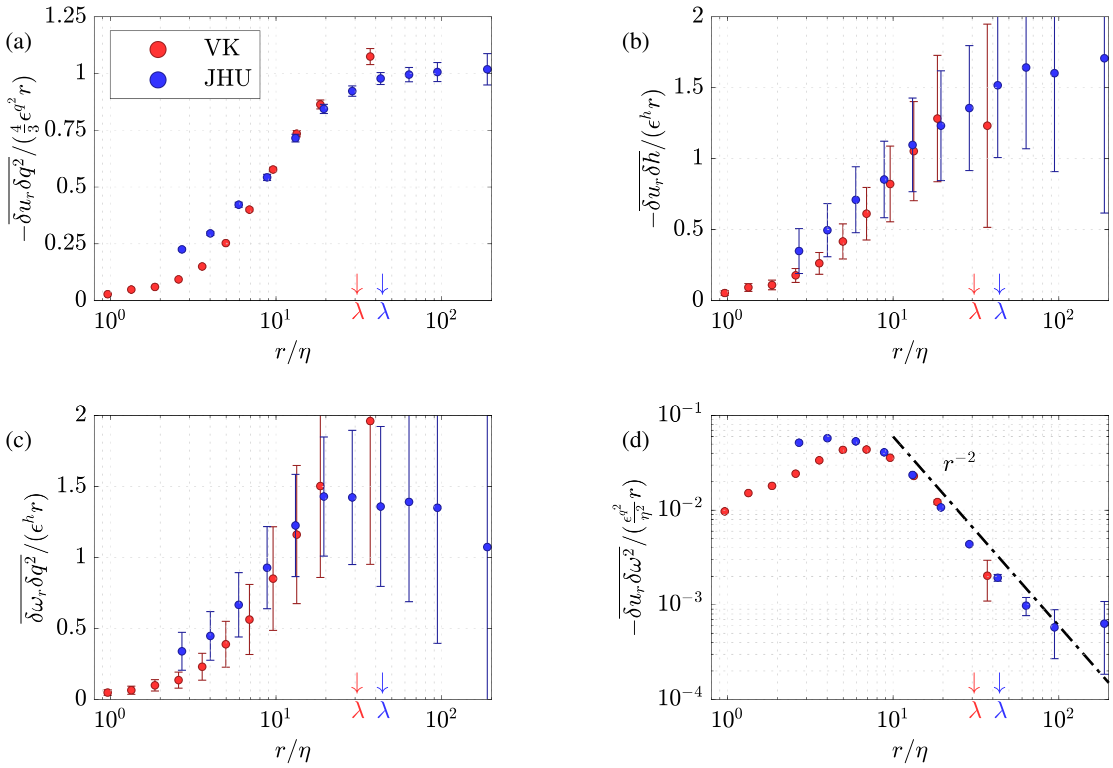

Figure 2: Normalised orientation-averaged NLF structure functions corresponding to the non-linear scale-to-scale flux of energy $\overline{\delta q^2}$ (a), helicity $\overline{\delta h}$ via advection (b) and vortex stretching (c), and enstrophy $\overline{\delta \omega^2}$ (d).

linear flux of helicity is very slow to converge, leading to large uncertainty bars. Despite this, they are found to be non-zero and the JHU data exhibits a plateau (within large uncertainty) for both non-linear helicity flux mechanisms.

Finally, the NLF enstrophy structure functions can be seen in fig. 2(d) normalised using the dissipation rate of energy, the Kolmogorov length scale η, and r. Similarly to the enstrophy structure function, a collapse of the data sets is observed in the near-dissipation range between $r/\eta = 10$ and $r/\lambda = 1$. The flux is seen to decrease as r^{-3} (r^{-2} in the figure due to compensating $-\overline{\delta u_r \delta \omega^2}$ by r) into the inertial range. This power law decrease is consistent with the results of Davidson *et al.* (2008) (in their case, an alternative scale-by-scale enstrophy flux is defined that is not motivated by the present spherical scale-space coordinate system. This necessitates compensating $-\overline{\delta u_r \delta \omega^2}$ by r for a one-to-one comparison).

Correlations of Instantaneous Cascades

In the following we consider the correlations within the cascades (i.e. terms of equations 1-3 individually) and between cascades (i.e. terms across equations 1-3). We focus on the separation $r = \lambda$, the Taylor microscale, as this is the upper bound for scales conditioned by viscosity (Yasuda & Vassilicos, 2018; Valente & Vassilicos, 2015).

Correlations within cascades The correlations of the transfer terms for the energy, helicity, and enstrophy

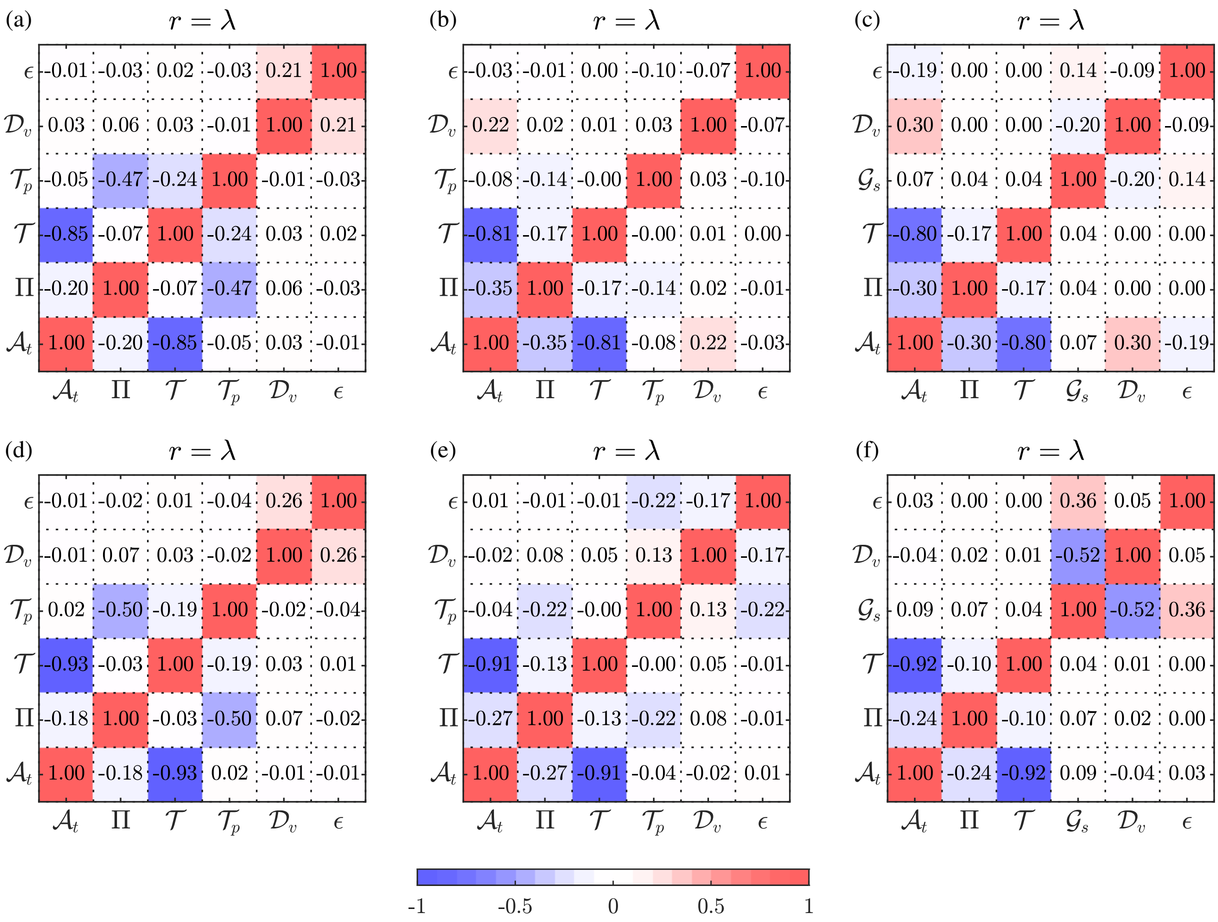

Figure 3: Correlation between various transfers of scale-space energy δq^2 (a) & (d), helicity δh (b) & (e), and enstrophy $\delta\omega^2$ (c) & (f) for the experimental VK data (a)-(c) and the DNS of JHU (d)-(f) at the scale $r = \lambda$.

cascades are presented in figure 3. Starting with the energy, the correlations of terms are in good agreement between both the JHU and VK data. The most robust correlation lies between the unsteady transport $\mathscr{A}_t^{q^2}$ and the turbulent transport $\mathscr{T}^{q^2}$. Recalling that $\mathscr{T}$ is associated with transport in physical space X_k, the high correlation between $\mathscr{A}_t^{q^2}$ and $\mathscr{T}^{q^2}$ is characteristic of the advective nature of turbulence. This is known from single-point analysis as the random sweeping effect and extends to scale space (Yasuda & Vassilicos, 2018). As explained by Tsinober (2001), it is caused by the tendency of the unsteady acceleration of the NS equations $\frac{\partial}{\partial t}u_i$ to anti-align with the convective acceleration $u_k\frac{\partial}{\partial x_k}u_i$, with increasing anti-alignment for increasing Reynolds number.

It should be noted that the random sweeping effect is, more accurately, represented by the correlation between $\mathscr{A}_t^{q^2}$ and the difference $\mathscr{T}^{q^2} - \Pi^{q^2}$ (Yasuda & Vassilicos, 2018). Nevertheless, the present analysis is restricted to correlations between individual terms of equation 1. Despite this difference, a strong individual correlation with $\mathscr{T}^{q^2}$ is observed, consistent with the results of Yasuda & Vassilicos (2018).

Turning attention to the non-linear transfer Π^{q^2}, a significant anti-correlation between Π^{q^2} and the pressure transport $\mathscr{T}_p^{q^2}$ is clear. Yasuda & Vassilicos (2018) used geometric analysis to show that this is due to the tendency of δu_i and $\delta\frac{\partial p}{\partial x_i}$ to align in such a way that compressing motions move energy downscale and stretching motions upscale. Although the opposite happens too (e.g. compressing upscale and stretching downscale), the overall tendency is for the pressure transport to facilitate downscale energy transfer. The non-local nature of the pressure field (Tsinober, 2001) and its resulting influence on transport motivates the interpretation of this correlation as a signature of non-locality on the non-linear energy transfer. Despite the difference in domain and boundary conditions, for the energy cascade the agreement in the correlation of $\mathscr{T}_p^{q^2}$ and Π^{q^2} between the two data sets is high.

The correlations of the transfer terms of the scale to scale helicity reveal that the same mechanisms within the energy cascade are present in the helicity cascade. The random sweeping effect is evident from the correlation between $\mathscr{A}_t^h$ and $\mathscr{T}^h$, being only slightly lesser in magnitude when compared to the corresponding terms for the energy. In contrast to the energy, the pressure transport $\mathscr{T}_p^h$ appears to have only a weak correlation with the non-linear transfer Π^h. If the same picture holds here as for the energy cascade, this indicates the non-local role played by the pressure in facilitating the non-linear cascade of helicity is not as significant at $r = \lambda$.

For the scale to scale enstrophy transfers, due to the "curling out" of the pressure transport, instead a generation term $\mathscr{G}_s^{\omega^2}$ features in equation 3. Caution must be exercised in interpreting the results for the enstrophy transfers. Noise propagation in the VK data renders correlations of $\mathscr{A}_t^{\omega^2}$ and $\mathscr{E}^{\omega^2}$ particularly erroneous. As a result in the following we focus on the results of the JHU data in figure 3(f).

A striking similarity with the energy and helicity cascades is immediately apparent through the anti-correlation of the un-

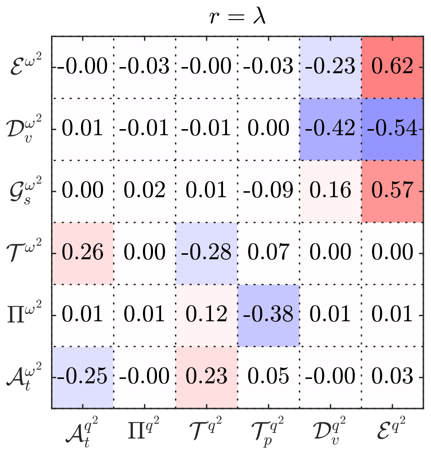

Figure 4: Correlation coefficients between terms of equations 1 and 3 (respectively transfers terms of δq^2 and $\delta\omega^2$ on the horizontal and vertical axis) at $r = \lambda$ in the JHU data.

steady transport $\mathscr{A}_t^{\omega^2}$ and turbulent transport $\mathscr{T}^{\omega^2}$. This confirms that the random sweeping effect persists across cascades. The generation term $\mathscr{G}_s^{\omega^2}$ has a different instantaneous role in the transfers of the enstrophy compared to the role of the pressure transport in energy and helicity. It exhibits a positive correlation with $\mathscr{E}^{\omega^2}$ and a negative correlation with $\mathscr{D}_v^{\omega^2}$. This implies a concurrent enstrophy generation and dissipation mechanism (Davidson *et al.*, 2008). This simultaneous generation and dissipation is tied to a reduction (during high dissipative events) or increase (during low dissipative events) in the diffusion of enstrophy.

Correlations between cascades Correlations between transfers of energy and helicity and between transfers of enstrophy and helicity were computed and found to be universally near zero. This is due to the non positive definiteness of helicity (Moffatt & Tsinober, 1992). At first glance, this appears to contradict a wealth of research that has identified clear causal relationships between the three quantities (Bershadskii *et al.*, 1994; Biferale *et al.*, 2013; Alexakis, 2017; Bos, 2021). As discussed by Tsinober (2001), near-zero correlations are necessary, but not sufficient, to determine that quantities are unrelated. For example, the unsteady term $\frac{\partial u_i}{\partial t}$ is almost entirely decorrelated with the material acceleration $\frac{Du_i}{Dt}$ simply due to the underlying anti-correlation of $\frac{\partial u_i}{\partial t}$ with $u_k\frac{\partial u_i}{\partial x_k}$.

Correlations between the transfers of energy and enstrophy are not affected by non positive definiteness and are shown for the JHU data in figure 4. The most robust correlation appears in the dissipation, where the rate of energy dissipation $\mathscr{E}^{q^2}$ and the rate of enstrophy dissipation $\mathscr{E}^{\omega^2}$ are highly correlated. Following from this correlation between the dissipations, there is a negative correlation between energy dissipation $\mathscr{E}^{q^2}$ and enstrophy diffusion $\mathscr{D}_v^{\omega^2}$ and a positive correlation between energy dissipation $\mathscr{E}^{q^2}$ and enstrophy generation $\mathscr{G}_s^{\omega^2}$. Together, this supports the classical picture that the generation of small-scale structures leads to large gradients and in turn the dissipation of energy (as well as enstrophy generation, Siggia, 1981).

Several other observations are of note between the energy and enstrophy cascades. The signature of the random sweeping effect can be clearly seen amongst the weak correlations between $\mathscr{A}_t$ and $\mathscr{T}$. There is a positive correlation between the transient energy $\mathscr{A}_t^{q^2}$ and the turbulent transport of enstrophy $\mathscr{T}^{\omega^2}$ (and vice-versa). Consider the turbulent transport of enstrophy expressed as $\mathscr{T}^{\omega^2} = \frac{1}{2}\Sigma u_k \frac{\partial}{\partial X_k}\delta\omega^2$. When Σu_k aligns with the physical space gradient of the scale enstrophy $\frac{\partial}{\partial X_k}\delta\omega^2$, the turbulent transport is positive. The sweeping motions (embodied by Σu_k) *assist* the scale enstrophy gradient (in other words, they sweep *with* the gradient). When Σu_k anti-aligns with $\frac{\partial}{\partial X_k}\delta\omega^2$, the sweeping motions *resist* the scale enstrophy gradient. Consider also the close relationship between the dissipation of energy and the scale enstrophy. Together, the positive correlation of $\mathscr{T}^{\omega^2}$ and $\mathscr{A}_t^{q^2}$ relates to energy decay for sweeping motions *assisting* the physical space gradient of the dissipation of energy. Similarly, it corresponds to energy growth for sweeping motions *resisting* the physical space gradient of the dissipation of energy. This effect is mirrored by the positive correlation of $\mathscr{T}^{q^2}$ and $\mathscr{A}_t^{\omega^2}$. This hints at the significance of the alignment of sweeping motions with the scale velocity gradients of the flow.

An anti-correlation between the unsteady terms $\mathscr{A}_t^{q^2}$ and $\mathscr{A}_t^{\omega^2}$ is also observed, with increasing anti-correlation for decreasing scale. This implies that instantaneous enstrophy growth corresponds to energy decay (and vice-versa). If we again consider that the enstrophy positively correlates to the dissipation of energy, this anti-correlation is interpreted as simply the tendency for the energy to decay when the local dissipation is growing in time (and vice versa). This is unsurprising considering the role of the dissipation as a sink. Due to the tendency of $\partial u_i/\partial t$ to anti-align with $u_k\frac{\partial}{\partial x_k}u_i$ (the random sweeping effect), the same phenomenon follows for the anti-correlation of $\mathscr{T}^{q^2}$ and $\mathscr{T}^{\omega^2}$.

CONCLUSIONS

We have presented an instantaneous analysis of the simultaneous energy, helicity, and enstrophy cascades of forced homogeneous incompressible turbulence focusing on the separation at the Taylor microscale. The scale-space framework, already well established for generalisation of the energy cascade via the KHMH equation, has been extended analogously to the scale-space helicity and enstrophy. It was found that large-scale sweeping is present across the three cascades: this is identified through the significant anti-correlation of the transient and physical-space transport terms of each cascade. In addition, the correlation between the pressure and inter-scale transfer terms, already reported by Yasuda & Vassilicos (2018) in the context of the energy cascade, is observed in the helicity cascade. The energy and enstrophy cascades are found to correlate with each other mostly through the generation/dissipation of enstrophy and dissipation of kinetic energy. The signature of the random sweeping mechanism is also identified between them. The present work represents a rich framework for future analyses of turbulence cascades in scale space coordinates.

ACKNOWLEDGEMENTS

The authors are indebted to B. Ganapathisubramani for supporting this work and enabling its dissemination at TSFP 12.

REFERENCES

Alexakis, Alexandros 2017 Helically decomposed turbulence. *Journal of Fluid Mechanics* **812**, 752–770.

Alves Portela, F, Papadakis, G & Vassilicos, JC 2017 The turbulence cascade in the near wake of a square prism. *Journal of Fluid Mechanics* **825**, 315–352.

Bershadskii, A, Kit, E, Tsinober, A & Vaisburd, H 1994 Strongly localized events of energy, dissipation, enstrophy and enstrophy generation in turbulent flows. *Fluid dynamics research* **14** (2), 71.

Biferale, L, Musacchio, Stefano & Toschi, F 2013 Split energy-helicity cascades in three-dimensional homogeneous and isotropic turbulence .

Bos, Wouter JT 2021 Three-dimensional turbulence without vortex stretching. *Journal of Fluid Mechanics* **915**.

Chen, Qiaoning, Chen, Shiyi & Eyink, Gregory L 2003 The joint cascade of energy and helicity in three-dimensional turbulence. *Physics of Fluids* **15** (2), 361–374.

Chkhetiani, OG 1996 On the third moments in helical turbulence. *Journal of Experimental and Theoretical Physics Letters* **63** (10), 808–812.

Davidson, PA, Morishita, K & Kaneda, Y 2008 On the generation and flux of enstrophy in isotropic turbulence. *Journal of Turbulence* (9), N42.

Germano, Massimo, Piomelli, Ugo, Moin, Parviz & Cabot, William H 1991 A dynamic subgrid-scale eddy viscosity model. *Physics of Fluids A: Fluid Dynamics* **3** (7), 1760–1765.

Gomes-Fernandes, R, Ganapathisubramani, B & Vassilicos, JC 2015 The energy cascade in near-field non-homogeneous non-isotropic turbulence. *Journal of Fluid Mechanics* **771**, 676–705.

Goto, Susumu & Vassilicos, JC 2016 Unsteady turbulence cascades. *Physical Review E* **94** (5), 053108.

Hill, Reginald J 2002 Exact second-order structure-function relationships. *Journal of Fluid Mechanics* **468**, 317–326.

Knutsen, Anna N, Baj, Pawel, Lawson, John M, Bodenschatz, Eberhard, Dawson, James R & Worth, Nicholas A 2020 The inter-scale energy budget in a von kármán mixing flow. *Journal of Fluid Mechanics* **895**.

Kolmogorov, Andrey Nikolaevich 1941*a* Dissipation of energy in locally isotropic turbulence. In *Dokl. Akad. Nauk SSSR*, , vol. 32, pp. 16–18.

Kolmogorov, Andrey Nikolaevich 1941*b* The local structure of turbulence in incompressible viscous fluid for very large reynolds numbers. In *Dokl. Akad. Nauk SSSR*, , vol. 30, pp. 299–303.

Levich, E & Shtilman, L 1988 Coherence and large fluctuations of helicity in homogeneous turbulence. *Physics Letters A* **126** (4), 243–248.

Li, Yi, Perlman, Eric, Wan, Minping, Yang, Yunke, Meneveau, Charles, Burns, Randal, Chen, Shiyi, Szalay, Alexander & Eyink, Gregory 2008 A public turbulence database cluster and applications to study lagrangian evolution of velocity increments in turbulence. *Journal of Turbulence* (9), N31.

L'vov, Victor S, Podivilov, Evgenii & Procaccia, Itamar 1997 Exact result for the 3rd order correlations of velocity in turbulence with helicity. *arXiv preprint chao-dyn/9705016* .

Mininni, PD, Alexakis, A & Pouquet, Annick 2006 Large-scale flow effects, energy transfer, and self-similarity on turbulence. *Physical Review E* **74** (1), 016303.

Moffatt, HK & Tsinober, A 1992 Helicity in laminar and turbulent flow. *Annual review of fluid mechanics* **24** (1), 281–312.

Mollicone, J-P, Battista, F, Gualtieri, P & Casciola, CM 2018 Turbulence dynamics in separated flows: The generalised kolmogorov equation for inhomogeneous anisotropic conditions. *Journal of Fluid Mechanics* **841**, 1012–1039.

Richardson, Lewis Fry 1920 The supply of energy from and to atmospheric eddies. *Proceedings of the Royal Society of London. Series A, Containing Papers of a Mathematical and Physical Character* **97** (686), 354–373.

Siggia, Eric D 1981 Numerical study of small-scale intermittency in three-dimensional turbulence. *Journal of Fluid Mechanics* **107**, 375–406.

Tsinober, Arkady 2001 *An informal introduction to turbulence*, , vol. 63. Springer Science & Business Media.

Valente, PC & Vassilicos, JC 2015 The energy cascade in grid-generated non-equilibrium decaying turbulence. *Physics of Fluids* **27** (4), 045103.

Yan, Zheng, Li, Xinliang, Yu, Changping & Chen, Shiyi 2019 Dual channels of helicity cascade in turbulent flows. *arXiv preprint arXiv:1907.03634* .

Yasuda, Tatsuya & Vassilicos, John Christos 2018 Spatio-temporal intermittency of the turbulent energy cascade. *Journal of Fluid Mechanics* **853**, 235–252.